Efficient and Repetitive Neutron Generation by Double-Laser-Pulse Driven Photonuclear Reaction[*)]

Yasunobu ARIKAWA, Yusuke KATO, Yuki ABE, Shuto MATSUBARA, Hidetaka KISHIMOTO, Nozomi NAKAJIMA, Alessio MORACE, Akifumi YOGO, Hiroaki NISHIMURA, Mitsuo NAKAI, Shinsuke FUJIOKA, Hiroshi AZECHI, Kunioki MIMA[1)], Shunsuke INOUE[2)], Yoshihide NAKAMIYA[2)], Kensuke TERAMOTO[2)], Masaki HASHIDA[2)] and Shuji SAKABE[2)]

Institute of Laser Engineering, Osaka University, 2-6 Yamadaoka, Suita, Osaka 565-0871, Japan
[1)]The Graduate School for the Creation of New Photonics Industries, 1955-1 Kurematsu-cho, Nishi-ku, Hamamatsu, Shizuoka 431-1202, Japan
[2)]Advanced Research Center for Beam Science, Institute for Chemical Research, Kyoto University, Gokasho, Uji, Kyoto 611-0011, Japan

(Received 25 August 2017 / Accepted 3 December 2017)

A short and high-intensity neutron pulse can be produced efficiently by using photonuclear reactions caused by Bremsstrahlung hard X-rays in a lase-irradiated high-Z target. The efficient and repetitive neutron generation was demonstrated with the combination of 1 Hz, 0.5 J, 25 fs, 5×10^{19} W/cm^2 laser pulses and a rotating tungsten disc targe. Here we applied double laser pulse irradiation scheme to increase the neutron generation efficiency. The first low-intensity laser pulse produces a lon-scale unde-critical-density plasma on the tungsten target surface prior to the second pulse irradiatio. High energy electrons above the ponderomotive scaling value are accelerated by the second hig-intensity pulse in the preformed plasm, this results in the increment of hard X-ray photons and photonuclear neutron. 3.5×10^4 neutron/pulse was obtained with optimized laser irradiation conditions.

Keywords: laser driven neutron source, high intensity laser, photonuclear reaction, relativistic electron acceleration

DOI: 10.1585/pfr.13.2404009

1. Introduction

High intensity, controllable, and safe neutron source is required for fundamental science, industry and medical applications, for example, laboratory experiments to study S-processes and R-processes occurred in the astronomical objects [1], a nondestructive inspection of massive structures [2], and neutron capture therapy [3].

The nuclear fission reactor is one of the neutron source facilities, however, there are rigorous regulations to construct, operate, maintain, and shut down the reactor safely. Accelerator based neutron source facility is developed as an alternative of the reactor. Although this type facility is more stable, controllable, and safe compared to the reactor, this facility is still large and expensive for the on-site non-destructive inspection application. The laser-based neutron source is receiving much attentions owing to its compactness, high peak intensity, and short pulse duration, despite the average neutron intensity being significantly lower than that obtained in the other facilities [4]. Repetitive neutron generation is essential for some applications that require not only high peak intensity but also high average flux of the neutron beam.

Several authors reported laser-driven neutron generations [5] based on nuclear fusion reactions by laser-driven implosion [6, 7], nuclear interactions of light atoms with protons and/or deuterons accelerated by high-intensity laser pulse [8, 9], and photonuclear reactions of matters with high energy photons generated by laser-matter interactions [10, 11]. National Ignition Facility (NIF), which is the world largest laser facility delivering up to 1.8 MJ of laser energy, achieved more than 10^{16} neutron yield per pulse by deuterium and tritium nuclear fusion reactions [6]. More efficient neutron generation (10^{11} of neutron yield per pulse) was demonstrated by using energetic particles accelerated by a relatively small 80-J single-shot laser system [8]. This scheme requires stable operation of ultra-high pulse contrast (better than 10^{11}). Continuous target supply is also a crucial issue for repetitive neutron generation. Gaseous deuterium clusters were used for this purpose [12], however a gas injection system and an evacuation pumping system for flammable deuterium gas is required. In this paper, we report the efficient and repetitive neutron generation owing to enhancement of photonuclear reactions by irradiating a rotating high-Z solid disc target with double laser pulses. The photonuclear reaction based neutron generation does not require high-contrast

author's e-mail: arikawa-y@ile.osaka-u.ac.jp
[*)] This article is based on the presentation at the Conference on Laser Energy Science / Laser and Accelerator Neutron Sources and Applications 2017.

laser pulse, thin foil or gaseous target, this is an advantage of this scheme for the industrial applications.

2. Method

Figures 1 (a) and (b) show a schematic drawing of the neutron generation and curves of photonuclear reaction cross section of various materials. The curves are referred from the JENDL database [13]. The neutron source consists of two parts as shown in Fig. 1 (a), one is a Bremsstrahlung x-ray generator and the other is a converter from X rays to neutrons by photonuclear reactions. High-intensity short-pulse laser is tightly focused on the x-ray generator made of a 1-mm-thick tungsten, in which laser-accelerated relativistic electrons are converted to Bremsstrahlung X-rays. The neutron generator is made of a 5 cm-thick lead. Lead has the largest cross sections among the candidates as shown in Fig. 1 (b) and is a stable and inexpensive material.

As shown in Fig. 1 (b), the photonuclear reaction of a lead has the sharp threshold at 12 MeV of photon energy. Increment of photon number in the energy range above 12 MeV is essential to increase neutrons by photonuclear reactions. The X-ray photons are generated by Bremsstrahlung process in the x-ray generator, therefore > 12 MeV electrons must be increased to increase > 12 MeV photons.

A Ti-Sapphire laser system [14], delivering 440-mJ of laser energy at 800-nm central wavelength was used in this experiment. The amplified chirped pulse was shortened with a grating pair to 25 fs of full width at half maximum (FWHM), and the laser beam was focused on a target with a $F/2$ parabola mirror to 2 - 3 μm of FWHM diameter spot. Maximum laser intensity was 5×10^{19} W/cm^2 on the target.

Mean energy of electrons accelerated by a 5×10^{19} W/cm^2 laser pulse is 1.2 MeV according to the ponderomotive scaling [15], this is too low to cause the photonuclear reactions in a lead. The previous studies [16, 17] indicate that energetic electrons, whose energies are above the ponderomotive scaling value, are produced in an under-dense plasma, whose electron density is lower than the critical density for the incident light. Preproduction of a long-scale under-dense plasma can increase the number of > 12 MeV electrons and this results in the increment of photonuclear neutrons. A Nd:YAG laser system having 1064-nm of wavelength, 25-mJ of pulse energy, 5 ns of FWHM pulse duration, and 4.5×10^{11} W/cm^2 of intensity was focused on the tungsten target with 25 μm of spot FWHM at 2 ns before the high-intense laser irradiation for producing a long-scale under-dense plasma.

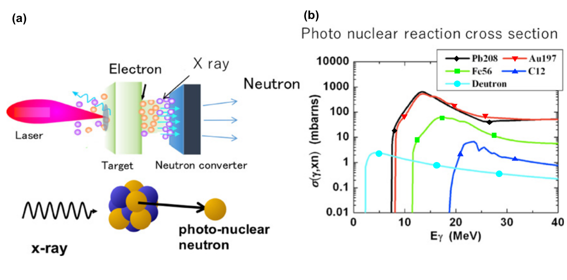

Fig. 1 (a) Schematic drawing of the neutron production scheme. (b) Cross section curves of photonuclear reaction for various materials.

3. Modelling of the Experiment

One-dimensional Particle-in-Cell (1D-PIC) simulation code (FISCOF 1D [18] was used for evaluating density scale length required for > 12 MeV electron production. Figure 2 (a) shows initial density profiles used in the

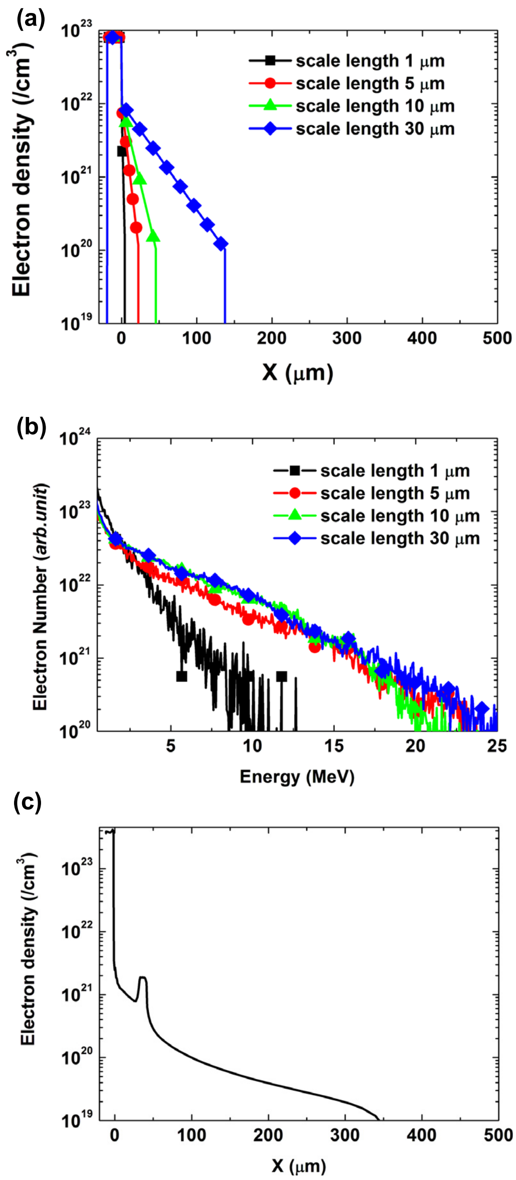

Fig. 2 (a) Initial density profiles for 1D-PIC simulation, (b) Electron energy distribution for various density scale length of the under-dense plasma, (c) Electron density profile of a long-scale under-dense plasma calculated by a 1D hydrodynamic simulation code (ILESTA-1D). A peak is corresponding a critical density for 1064 nm laser where laser is absorbed.

calculations, under-dense plasmas having exponential density profiles, whose scale length are 1, 5, 10 and 30 μm, are put on the surface of the solid density plasma. Figure 2 (b) shows the electron energy distribution calculated for 1, 5, 10 and 30 μm of density scale lengths. The laser field accelerates energetic electrons in the density range from 1/10 to 1 of the critical density. The calculations reveal that more than 5 μm of scale-length is necessary to produce > 12 MeV electrons. Figure 2 (c) shows a density profile produced by the first low-intensity laser pulse at 2 ns after the first pulse irradiation. This density profile was calculated by a 1D radiation-hydrodynamic simulation code (ILESTA-1D) with the experimental parameters. The calculation shows that the 0.1 critical density position moved about 80 μm away from the initial target surface. Focal position of the second high-intense laser pulse must be offset about 80 μm to obtain high intensity enough to accelerate energetic electrons in the under-dense plasma because the Rayleigh length of the second laser pulse is 8 μm.

4. Experiment

Figures 3 (a) and (b) show experimental setup for the electron energy distribution measurement and the neutron production.

A 10-μm thick tungsten target was irradiated by the double laser pulses. Energy distributions of the accelerated electrons were measured by an electron spectrometer (ESM) placed behind the target along the second laser axis. The electron energy distributions were measured by changing the target positions along the second laser axis from 0 to 200 μm to the second laser incident direction as shown in Fig. 4 (a). The significant increment of the high energy electrons was observed by irradiating the first low-intensity laser pulse on the target. Number of the electrons increases by enlarging the offset distance up to 80 μm and drops with larger than 100 μm. The number of electrons in higher energy part (over 8 MeV to 12 MeV which is detection limit) was also plotted in Fig. 4 (b).

A rotating 1-mm thick tungsten disc target was used to generate repetitively neutrons. Every laser pulse is illuminated on a pristine surface of the rotating disc target. A lead block with a size of 5 cm × 5 cm × 10 cm was put behind the disc target with a distance of 3 mm as a neutron convertor (Fig. 4 (b)). Absolutely calibrated neutron bubble detectors (BDS 1000), which are sensitive to > 1 MeV neutrons, were placed around the neutron convertor to measure the neutron yield. One of the bubble detectors was placed behind a 9-cm paraffin block to confirm that the neutron was generated at the neutron convertor by attenuating neutrons come from the convertor. The detectors were exposed to 1000 laser shots. Neutron yield was obtained from number of bubbles generated in the detectors with the assumption of isotropic neutron emanation. Neutron yields per shot were plotted for several offset positions (Fig. 5). 18 bubbles were observed at the maximum. The neutron signal of the bubble detector behind the paraffin was 1/9 of the others which is consistent with the calculated neutron attenuation rate (11% for 1 MeV neutrons), this indicates the neutrons were generated from the neutron convertor. The plots of neutron yield with a function of offset was consistent with the trend of the high energy electron generation as shown in Fig. 4 (b). The double pulse technique enhances the efficiency of the neutron generation. This scheme can be applied to higher repetitive laser, this work successfully demonstrates a promising method

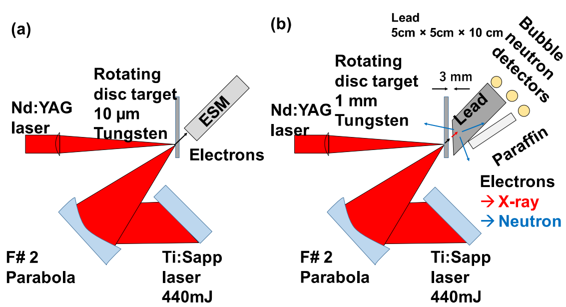

Fig. 3 Experimental set up for (a) electron measurement and (b) neutron production.

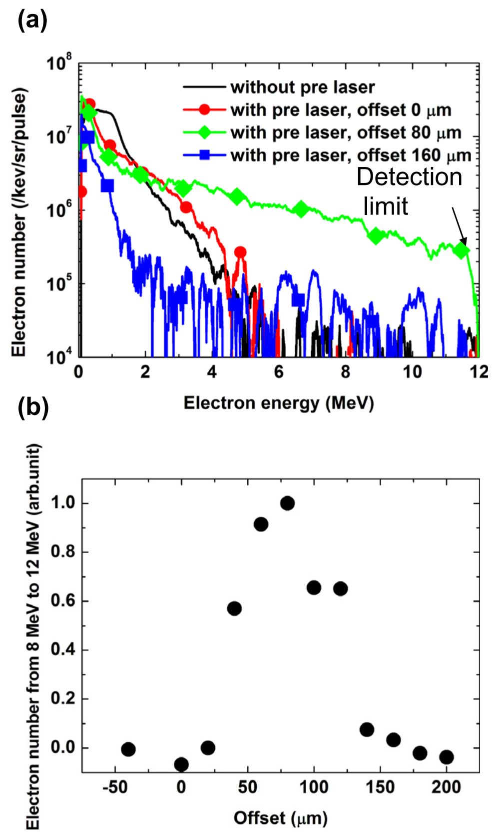

Fig. 4 (a) Electron energy distribution detected from the laser incident axis direction with the function of the offset of the target position from the laser focal one. The ESM with an aperture size 1 mm diameter was placed 100 mm from the target. (b) The number of electrons from 8 MeV to 12 MeV with the function of the offset.

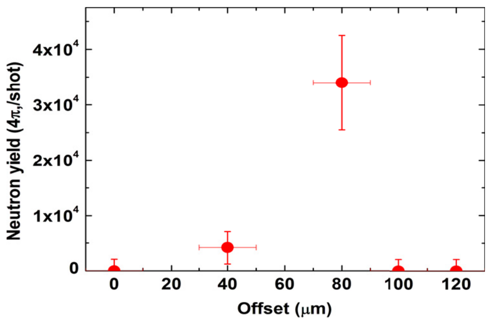

Fig. 5 Neutron yield with the function of the offset of the target position from the laser focal one.

of a repetitive laser-driven neutron source.

5. Summary

Repetitive generation of laser-driven neutron was demonstrated by using the combination of a 0.44-J table-top high-intense laser and a rotating tungsten disc target. The rotating tungsten disc target was irradiated by a 25 mJ 5-ns laser pulse to produce a long-scale under-dense plasma prior to the high intensity laser pulse irradiation. Energetic electrons above the ponderomotive scaling value were accelerated by the high intensity pulse in the preformed plasma. Energetic electrons are converted to x-rays by Bremsstrahlung process, which in turn are converted to neutrons via photonuclear reactions. 3.5×10^4 neutron/pulse were achieved with this scheme. Based on this experimental result, we will be able to demonstrate $> 10^7$ neutrons per second, which is high enough for the neutron radiography applications, with 10 J/10 Hz Ti:Sapphire laser system in the near future.

Acknowledgement

This work is supported by Adaptable Seamless Technology transfer Program through target driven R&D (A-STEP) of Japan Science and Technology Agency, Promotion of Science under the contracts of Grant-in-Aids for Scientific Research [Nos. 24244095, 2624043, 23360413, 16H02245], for Young Scientists [Nos. 24686103, 24684044], for Challenging Exploratory Research [Nos. 25630419, 16K13918], for the JSPS fellows [No. 14J06592], and the auspices of the Japanese Ministry of Education, Culture, Sports, Science and Technology (MEXT) project on "Promotion of relativistic nuclear physics with ultra-intense laser", and NIFS collaboration research program [NIFS12KUGK057, NIFS12KUGK070, NIFS11KUGK 053, NIFS15KUGK087].

[1] M. Burbidge, G.R. Burbidge, W.A. Fowler and F. Hoyle, Rev. Mod. Phys. **29**(4), 547 (1957).
[2] P. von Der Hardt and H. Rotger eds., *Neutron Radiography Handbook* (D. Reidel Publishing Company, Dordrecht, 1981).
[3] G.L. Locher, Am. J. Roentgenol. **36**, 1 (1936).
[4] S. Nakai, K. Mima, Y. Kato, K. Tanaka, Y. Ikeda, H. Azechi, K. Miyanaga, M. Nakai, M. Perlado and R. Gonzalez Arrabal, J. Phys. Conference Series **244**, Part 4 (2010).
[5] L.J. Perkins, B.G. Logan, M.D. Rosen, M.D. Perry, T. Diaz de la Rubia, N.M. Ghoniem, T. Ditmire, P.T. Springer and S.C. Wilks, Nucl. Fusion **40**, No. 1, 1 (2000).
[6] O.A. Hurricane, D.A. Callahan, D.T. Casey *et al.*, Nature **506**, 343 (2014).
[7] C. Yamanaka and S. Nakai, Nature **319(6056)**, 757 (1986).
[8] M. Roth, D. Jung *et al.*, Phys. Rev. Lett. **110**, 044802 (2013).
[9] K.L. Lancaster, S. Karsch *et al.*, Phys. Plasmas **11**, 3404 (2004).
[10] I. Pomerantz *et al.*, Phys. Rev. Lett. **113**, 184801 (2014).
[11] Y. Arikawa *et al.*, Plasma Fusion Res. **10**, 2404003 (2015).
[12] T. Ditmire, J. Zweiback, V.P. Yanovsky, T.E. Cowan, G. Hays and K.B. Wharton, Nature **398**, 492 (1999).
[13] K. Shibata, O. Iwamoto, T. Nakagawa, N. Iwamoto, A. Ichihara, S. Kunieda, S. Chiba, K. Furutaka, N. Otuka, T. Ohsawa, T. Murata, H. Matsunobu, A. Zukeran, S. Kamada and J. Katakura, J. Nucl. Sci. Technol. **48(1)**, 1 (2011).
[14] S. Tokita, M. Hashida, S. Masuno, S. Namba and S. Sakabe, Optics Express **16(19)**, 14875 (2008).
[15] S.C. Wilks, W.L. Kruer, M. Tabak and A.B. Langdon, Phys. Rev. Lett. **69**, 1383 (1992).
[16] T. Johzaki *et al.*, Plasma Fusion Res. **2**, 041 (2007).
[17] Y. Arikawa *et al.*, Nucl. Fusion **57**, 066022 (2017).
[18] H. Sakagami *et al.*, Laser Part. Beams **24**, 191 (2006).